



PCCP

Transition-metal solvated-electron precursors: Diffuse and 3d electrons in $V(NH_3)_6^{0,\pm}$

Journal:	<i>Physical Chemistry Chemical Physics</i>
Manuscript ID	CP-ART-12-2018-007420.R2
Article Type:	Paper
Date Submitted by the Author:	02-Mar-2019
Complete List of Authors:	Almeida, Nuno M. S.; Auburn University, Chemistry and Biochemistry Pawlowski, Filip; Auburn University, Chemistry and Biochemistry Orti, J.Vincent; Auburn University Miliordos, Evangelos; Auburn University, Chemistry and Biochemistry

SCHOLARONE™
Manuscripts

Transition-metal solvated-electron precursors: Diffuse and 3d electrons in $V(\text{NH}_3)_6^{0,\pm}$

*Nuno M. S. Almeida, Filip Pawłowski, Joseph Vincent Ortiz and Evangelos Miliordos**

Department of Chemistry and Biochemistry, Auburn University, Auburn, AL 36849-5312, USA

AUTHOR INFORMATION

Corresponding Author

* E-mail: emiliord@auburn.edu

ABSTRACT. Ground and excited electronic states of $V(\text{NH}_3)_6^{0,\pm}$ complexes, investigated with *ab initio* electronic structure theory, consist of a $V(\text{NH}_3)_6^{2+}$ core with up to three electrons distributed over its periphery. This result extends the concept of super-atomic, solvated-electron precursors from alkali and alkaline-earth complexes to a transition metal. In the approximately octahedral ground state of $V(\text{NH}_3)_6$, three unpaired electrons occupy $3d_{xz}$, $3d_{yz}$ and $3d_{xy}$ (t_{2g}) orbitals of vanadium and two electrons occupy a diffuse $1s$ outer orbital. The lowest excitations involve promotion of diffuse $1s$ electrons to $1p$ or $1d$ diffuse orbitals, followed by a $3d$ ($t_{2g} \rightarrow e_g$) transition. $V(\text{NH}_3)_6^+$ is produced by removing a diffuse $1s$ electron, whereas the additional electron in $V(\text{NH}_3)_6^-$ populates a $1p$ diffuse orbital. The adiabatic ionization energy and electron affinity of $V(\text{NH}_3)_6$ equal 3.50 and 0.48 eV, respectively.

I. Introduction

Addition of small quantities of alkali or alkaline-earth elements to liquid ammonia yields solvated ions: electrons and cationic metal cores.¹⁻³ Other solvents, such as water, acetonitrile and methanol, are also able to separate electrons from metals.⁴⁻⁶ Saturated metal-ammonia solutions produce a bronze-colored metallic phase whose conduction electrons are scattered by $M(\text{NH}_3)_n^{q+}$ complexes.^{1, 7, 8} Magnetic measurements at intermediate concentrations suggest the presence of diverse paramagnetic or diamagnetic species.¹ Singlet-coupled pairs of solvated electrons may reside in peanut-like cavities.⁹ In solvated electron precursors (SEPs), electrons occupy diffuse orbitals on the periphery of $M(\text{NH}_3)_n^{q+}$ complexes. Anions, dimers or clusters of SEPs also may be formed.^{1, 10, 11}

Investigation of molecular electronic structure in SEPs provides another perspective on metal-ammonia materials.¹ *Ab initio* calculations on ground states of SEPs have revealed the presence of one or two peripheral electrons in an s-like diffuse orbital that is delocalized outside cores such as $\text{Li}(\text{NH}_3)_4^+$, $\text{Na}(\text{NH}_3)_4^+$, and $\text{Be}(\text{NH}_3)_4^{2+}$.¹⁰⁻¹² Low-lying excited electronic states involve diffuse p-, d-, and f-like orbitals that resemble those of conventional atomic structure. Nearly identical orderings of states in all three cases support an Aufbau principle for diffuse electrons that differs radically from the hydrogenic orbital series. Higher angular momentum orbitals are stabilized over s-type orbitals: the first three levels are denominated 1s, 1p and 1d. These are followed by 2s, 1f, 2p and 2d levels whose order may vary from one core to the next.¹⁰
¹¹ Spectral¹³ and calculated¹⁰ 1s→1p excitation energies of $\text{Na}(\text{NH}_3)_4$ agree within 0.08 eV.

Formation of SEPs by Be, whose single and double ionization energies are 9.3 and 27.5 eV respectively,¹⁴ suggests that transition metals with lower ionization energies (e.g. Sc-Co) also may be capable of forming SEPs. Four and six being respectively the most common coordination

numbers for Be and early 3d metal dications, octahedral complexes of transition metals appear to be reasonable candidates for SEP formation. Three-fold degeneracy in non-bonding 3d orbitals of octahedral complexes (i.e. t_{2g} in O_h symmetry) indicates that $3d^3$ or $3d^6$ configurations may be especially stable. Following the precedent of two diffuse electrons in a totally symmetric orbital seen in the Be case leads to consideration of a 3d metal with a total of five valence electrons: vanadium. Iron, the alternative with three more electrons also confined to tightly bound, radially nodeless 3d orbitals, is likely to require treatments of stronger electron correlation effects, whereas vanadium may be expected to produce a relatively simple, high-spin, single-configuration complex. The possible presence of unpaired 3d electrons in hexa-amino vanadium complexes raises the prospect of paramagnetic SEPs and related solvated-electron materials with unprecedented combinations of electronic and magnetic properties.

Calculations presented below on $V(NH_3)_n$ for $n=1-6$ and its positive ions establish that six ammonia ligands are necessary to stabilize the outer electronic shell structure of a SEP. In ground-state $V(NH_3)_6$, pentavalent vanadium retains three inner 3d (t_{2g}) electrons in a high-spin quartet and relinquishes two electrons to a diffuse 1s orbital. Transition-metal SEPs in highly concentrated vanadium-ammonia solutions, such as $V(NH_3)_6$, can release two outer electrons to the band structure of the solid while keeping intact magnetic moments generated by three unpaired, well-protected 3d electrons. Results on ground and excited states of $V(NH_3)_6^{0,\pm}$ confirm diffuse-electron Aufbau principles discovered for alkali and alkaline-earth SEPs and distinguish transitions between diffuse orbitals from those that involve $3d t_{2g} \rightarrow e_g$ promotions.

II. Computational Methods

Geometry optimizations and harmonic vibrational frequencies for $V(NH_3)_n^{0,\pm}$ ($n=1-5$) were performed at the unrestricted MP2 level of theory. Unrestricted Hartree-Fock spin contamination

never exceeds 0.01 a.u. For $n=6$, UMP2 optimizations were followed by B3LYP^{15, 16} reoptimizations and harmonic frequency estimates of zero-point energies. (See Electronic Supplementary Information, ESI.) The basis set for these calculations comprised cc-pVTZ for V and N and aug-cc-pVTZ for H.¹⁷⁻¹⁹ Extra diffuse functions on H (i.e. d-aug-cc-pVTZ) were added in calculations on excitation and electron binding energies.^{10, 11, 20}

Optimal geometries for $V(\text{NH}_3)_6^{0,+}$ bear no symmetry elements and render multi-reference calculations on their excited states prohibitively expensive. All ammonia ligands therefore were rotated around their V-N axes to impose C_{2v} symmetry (see Figure 1). Ground-state energies of C_1 and C_{2v} structures differ respectively by 0.41, 0.20 and 0.30 kcal/mol for the neutral quartet, cationic quintet and anionic quintet. The accuracy of vertical excitation and electron binding energies reported herein is affected only slightly by this simplification.

The present complete active space self-consistent field (CASSCF) wavefunctions allocate five electrons to fourteen orbitals: 3d ($t_{2g}+e_g$) valence and 1s, 1p, 1d diffuse orbitals. With C_{2v} symmetry, the active space includes six a_1 , three b_1 , three b_2 , and two a_2 orbitals. Electron propagator calculations on higher states demonstrated no need for more diffuse CAS orbitals.

Dynamic correlation described with CASPT2 using MOLPRO 2015.1 (RS2C)²¹ includes substitutions from all valence electrons of $V(\text{NH}_3)_6^{2+}$ except from the lowest six N 2s-like orbitals. For the cationic and neutral complexes, 40 and 41 electrons were correlated respectively. To remove possible divergences caused by intruder states, a level shift value of 0.2 a.u. and an IPEA (shift parameter for orbital energies) value of 0.25 a.u. were applied.^{22, 23}

Electron affinities of $V(\text{NH}_3)_6^{2+}$ at the $V(\text{NH}_3)_6^+$ structure were calculated with the renormalized partial third-order quasiparticle (P3+) electron propagator method;²⁴ vertical excitation energies for $V(\text{NH}_3)_6^+$ were inferred from their differences. Replacement of cc-pVTZ

with cc-pwCVTZ on V in MP2 and P3+ calculations yields only minor discrepancies in dicationic electron affinities. MP2 geometries optimizations, B3LYP frequencies and P3+ electron affinities were obtained with Gaussian 16.²⁵

III. Results and Discussion

IIIA. Ground State Calculations on $V(NH_3)_n^{0,\pm}$

The 4F ground state of vanadium arises from $4s^23d^3$ configurations and is followed by 6D , wherein one 4s electron is transferred to 3d. Their M_J -averaged energy difference is $1,977\text{ cm}^{-1}$.¹⁴ Doubly occupied 4s is expected to resist binding between V and NH_3 through repulsive interactions with the ligand's lone electron pairs. Despite a barrier to concerted coordination (see below), ammonia molecules make dative bonds with the positively charged vanadium core at the equilibrium geometry of $V(NH_3)_6$ (see Figure 2). Similar bonding schemes occur in lithium, sodium, and beryllium SEPs.^{10, 11} With each additional NH_3 ligand, 4s electrons are pushed to the periphery of the molecule. Figure 2 depicts the shape of the highest occupied molecular orbital (HOMO) of $V(NH_3)_{n=1-6}$ at the Hartree-Fock level. In all cases, the ground state is a quartet. For the same probability iso-surface (80%), the HOMO expands with the number of ligands and eventually encloses them. Finally, 4s of vanadium is transformed to the pseudo-spherical outer 1s orbital of $V(NH_3)_6$.

Figure 3 juxtaposes atomic V 4s, 4p, 5s and 5p with outer $V(NH_3)_6$ 1s and 1p orbitals on an axis defined by V and the center of an octahedral N-N-N face. The 1s orbital has a local maximum at $\sim 2.95\text{ \AA}$, the same number of nodes as V 4s and an extended tail that imply an accumulation of electron density on the outer periphery of N-H bonds. The 1s maximum lies inside the most diffuse extremum of the 5s orbital at $\sim 3.45\text{ \AA}$. There is a shoulder at $\sim 1.0\text{ \AA}$ that is near a local maximum of 4s. The 1p outer orbital has a diffuse maximum near the most diffuse extremum

of 5p, a shoulder near a local maximum of 4p, and an extended tail. For both diffuse orbitals, major distortions with respect to atomic orbitals occur with retention of the number of radial nodes. Similar observations were made for $\text{Be}(\text{NH}_3)_4$, where outer orbitals distort in response to the non-spherical electrostatic potential of a dicationic core.¹¹

Table 1 lists both the total ($D_{e,\text{tot}}$) and sequential (D_e) binding energies for all $\text{V}(\text{NH}_3)_{n=1-6}$ complexes. D_e follows an alternating pattern of small and large values ranging from 5.1 ($n = 3$) to 25.2 ($n = 6$) kcal/mol. The total binding energy sums up to 94.2 kcal/mol for $\text{V}(\text{NH}_3)_6$ and amounts to 15.7 kcal/mol per V-NH₃ bond. Corresponding per-bond values for $\text{Li}(\text{NH}_3)_4$, $\text{Na}(\text{NH}_3)_4$, and $\text{Be}(\text{NH}_3)_4$ are 14.2, 8.0, and 16.0 kcal/mol, respectively.^{10, 11}

The M_J -averaged ground state of 5D ($3d^4$) V^+ is 2,720 cm^{-1} below 5F ($4s^1 3d^3$).¹⁴ This excitation from 3d to 4s is in the opposite direction compared to neutral vanadium. In the ground state of $\text{V}(\text{NH}_3)^+$, the singly occupied 4s orbital is similar to its monocoordinate counterpart in Figure 2. Ground states of all $\text{V}(\text{NH}_3)_n^+$ complexes are quintets. Vanadium ions in these complexes resemble their 5F antecedents with higher orbital angular momentum. Table 2 lists binding energies for the cationic complexes, which are larger than those of Table 1 for $n=1-4$. For $\text{V}(\text{NH}_3)_6^+$, the total binding energy is 166.7 kcal/mol, or 27.8 kcal/mol per V-NH₃ bond.

Stepwise addition of two diffuse 1s electrons to $\text{V}(\text{NH}_3)_6^{2+}$ yielding $\text{V}(\text{NH}_3)_6$ elongates N-H bonds by 0.003 Å or less, but shortens the V-N bond by 0.025 and 0.012 Å (see Table 3). Little structural change occurs in $\text{V}(\text{NH}_3)_6^-$ or $\text{Be}(\text{NH}_3)_4^-$ with the addition of a 1p electron.^{10, 11}

The P3+ vertical ionization energy and electron affinity of C_{2v} $\text{V}(\text{NH}_3)_6$ are 3.44 and 0.46 eV, respectively. MP2 corrections for geometric relaxation to C_1 structures and B3LYP zero-point energies imply that the adiabatic ionization energy and the electron affinity respectively amount to 3.50 and 0.48 eV (see Table 3). Similar corrections to the P3+ vertical electron affinity of the

dication calculated at the C_{2v} geometry of the cation (6.26 eV) enable determination of the adiabatic, relative energy of the dication (9.85 eV) with respect to $V(NH_3)_6$.

IIIB. Excited states of $V(NH_3)_6$

The first three electronic states of vanadium and their dominant configurations are: 4F ($4s^23d^3$), 6D ($4s^13d^4$), and 4D ($4s^13d^4$). In the concerted approach of six ammonia ligands to the metal center, retention of orbital symmetry would produce a dicationic core with two diffuse $1s$ electrons in the first case and a monocationic core with one diffuse $1s$ electron in the other two. These two possibilities are denoted by $V(NH_3)_6^{2+}:2e^-(1s^2)$ and $V(NH_3)_6^+:1e^-(1s^1)$, respectively. The $4s$ orbital would be transformed to the $1s$ outer one discussed in Section IIIA and shown in Figure 4. Antibonding interactions between $V 4s$ and NH_3 HOMOs would produce a larger barrier in curves that have a 4F dissociation limit.

Potential energy curves (PECs) for a concerted approach with equal V-N distances to the C_{2v} structure of Figure 1 put the orbital symmetry hypothesis to the test. Some PECs are nearly degenerate because of their approximately octahedral structure. Therefore, octahedral labels are used for electronic terms. CASSCF PECs are plotted in Figure 5. Because CASSCF incorrectly predicts a 6D ground state, more accurate PECs for sextets are shifted to higher energies, so that their asymptotic limits lie between those of 4F and 4D .

Figure 5's PECs confirm that energy barriers for $4s^1$ states ($^4,^6D$) are appreciably smaller than the $4s^2$ (4F) one; compare for example $^4A_{2g}$, 4E_g or $^6T_{2g}$ PECs. This effect generates the avoided crossing around $R = 3.5 \text{ \AA}$ for the two $^4T_{2g}$ states that pertain to 4D and 4F dissociation limits. Stabilization of $V(NH_3)_6^{2+}:2e^-(1s^2)$ over $V(NH_3)_6^+:1e^-(1s^1)$ states causes another avoided crossing for the two $^4T_{2g}$ states near $R = 2.7 \text{ \AA}$. $V(NH_3)_6^+:1e^-(1s^1)$ states have longer equilibrium

bond lengths (2.7-2.8 Å) than $V(NH_3)_6^{2+}:2e^-(1s^2)$ ones (2.3-2.5 Å) and repeat the trend seen for $Be(NH_3)_4^{0,+}$, where the $1s^2$ neutral complex has a shorter Be-N length than the $1s^1$ cation.¹¹

To overcome excessive stabilization of sextet states at the CASSCF level, dynamic correlation was included with MP2 optimizations for the single-reference lowest sextet (6E_g) state. An energy difference of 2.35 eV (54.2 kcal/mol) was obtained between $V(NH_3)_6^{2+}:2e^-(1s^2)$ ${}^4A_{2g}$ and $V(NH_3)_6^+:1e^-(1s^1)$ 6E_g minima. This value exceeds the highest energy of the $V(NH_3)_6^{2+}:2e^-(1s^2)$ states examined below. Therefore, $4s^2$ states are in general more stable than those with $4s^1$ character. Because the active space includes only $4s$ and $3d$ orbitals of vanadium, PECs of states that occupy higher, outer orbitals (see below) cannot be depicted in Figure 5.

CASSCF and CASPT2 excited-state energies at the optimal, pseudo-octahedral, C_{2v} structure for the ground ${}^4A_{2g}$ state of Figure 1 are tabulated in Table 4. All five $3d$ -like orbitals are illustrated in Figure 6 along with selected $1s$, $1p$ and $1d$ outer orbitals. The lowest excited states pertain to transitions between diffuse orbitals. The first $t_{2g} \rightarrow e_g$ transitions to ${}^4T_{2g}$ states occur at ~ 1.75 eV with CASPT2. No $3d \leftrightarrow$ diffuse transitions in the first forty-five states of $V(NH_3)_6$ up to approximately 2.0 eV were found. CASPT2 excitation energies are consistently larger by an averaged difference of $\delta E = 0.236$ eV. In cases where CASPT2 failed to converge, an estimated value is obtained by adding δE to the CASSCF result. A more detailed analysis on the electronic structure of the excited states is given in the ESI.

III C. Excited states of $V(NH_3)_6^{\pm}$

In the cation, spin coupling between t_{2g}^3 (${}^4A_{2g}$) and $1s^1$ (2S) generates ${}^3A_{2g}$ and ${}^5A_{2g}$ states which are practically degenerate. Table 5 lists vertical excitation energies at the optimized quintet's structure. CASSCF and P3+ favor ${}^5A_{2g}$ by ~ 0.015 eV, but CASPT2 favors ${}^3A_{2g}$ by only

0.004 eV. Close agreement between wavefunction and electron-propagator results confirms the one-electron character of the electron detachment from the ground state of $V(NH_3)_6$.

As in the neutral system, the first excited states exhibit $1s \rightarrow 1p$ promotion. Next, transitions within the 3d-shell occur, e.g. $t_{2g} \rightarrow e_g$ or t_{2g}^3 (quartet \rightarrow doublet). Finally, excitations from 1s to higher energy diffuse orbitals take place (1d, 1f, 2s, 2p). The higher excitations were feasible only with P3+. Representative Dyson orbitals for electron attachment to the dication in Figure 7 for quintet states are nearly unchanged for triplets.

CASPT2 predicts larger T_e values than CASSCF by an average of 0.053 eV for states with $t_{2g}^2 e_g^1$ (${}^4T_{2g}$) character. This correction may be added to the highest ${}^4T_{2g}$ state components of Table 4 for $V(NH_3)_6$, where CASPT2 calculations were not possible for its components. Consideration of V 3s and 3p electron correlation in geometry optimization and in P3+ calculations increases T_e values by only 0.015 eV or $\sim 1\%$, on average. A more detailed account is provided in the ESI.

The vertical electron detachment energy of $V(NH_3)_6^-$ calculated at the P3+ level is 0.46 eV. The ground state is a quintet ${}^5T_{2u}$ state of t_{2g}^3 (${}^4A_{2g}$) $1s^2 1p^1$ (2P) character, followed by its companion triplet ${}^3T_{2u}$, where the t_{2g}^3 quartet couples to 2P ($1p^1$) anti-ferromagnetically. All triplet and quintet components are practically degenerate. The ground state of V^- is 5D ($4s^2 3d^4$).²⁶ When six ammonia ligands attach to vanadium, the metal atom's $4s^2$ electrons become outer $1s^2$ ones while one of the 3d electrons migrates to the outer 1p orbital.

IV. Conclusions

Neutral, cationic and anionic hexa-amino vanadium complexes have been studied with high-level quantum chemical methodologies. The stability of their ground states has been confirmed by means of real harmonic vibrational frequencies and moderate binding energies with respect to ammonia dissociation channels. *Super-atomic character reported previously for alkali*

and alkaline-earth metal ammonia complexes has been demonstrated for a transition-metal complex. The electronic structure of ground and several low-lying excited states has been elucidated and accurate vertical excitation energies have been provided. Vanadium $3s^23p^6$ electron correlation has been found to have little net effect on excitations energies.

Ground-state $V(NH_3)_6$ is approximately octahedral and has three, quartet-coupled electrons residing in non-bonding, t_{2g} -like orbitals of vanadium plus two electrons occupying an outer s-like orbital that is markedly more diffuse than vanadium 4s. Alkali, alkaline-earth and transition-metal solvated-electron precursors have the same diffuse-orbital Aufbau principle: 1s, 1p, 1d, 2s, 1f, 2p. Excitations among the outer orbitals occur at lower energies. Inner, $t_{2g} \rightarrow e_g$ transitions are accessed only at energies that are larger than those for diffuse $1s \rightarrow 1d$ excitations. The same observations can be made for $V(NH_3)_6^+$, which has only one outer electron. The $V(NH_3)_6^-$ ground state has three outer electrons with a $1s^21p^1$ configuration and is bound by ~ 0.5 eV with respect to $V(NH_3)_6$.

Saturated vanadium-ammonia solutions should have well-protected, high-spin-coupled electrons at every metal center and thus are expected to exhibit large magnetic susceptibilities. Future work will aim at the study of more transition-metal ammonia complexes and highlight the trends observed along the first and second row of the d-block of the periodic table.

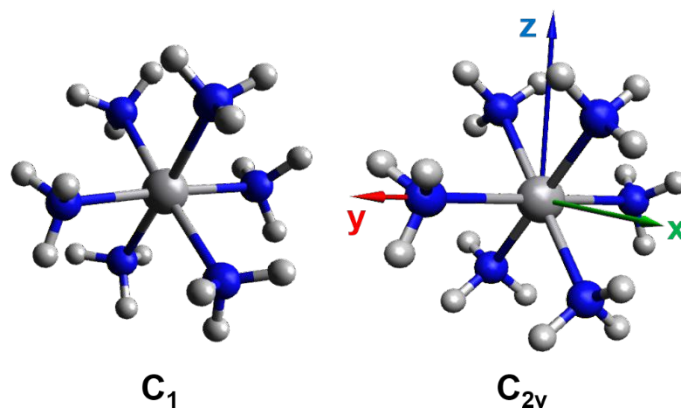


Figure 1. Optimal C_1 and C_{2v} $V(NH_3)_6$ structures. Note rotations of the two bottom NH_3 ligands.

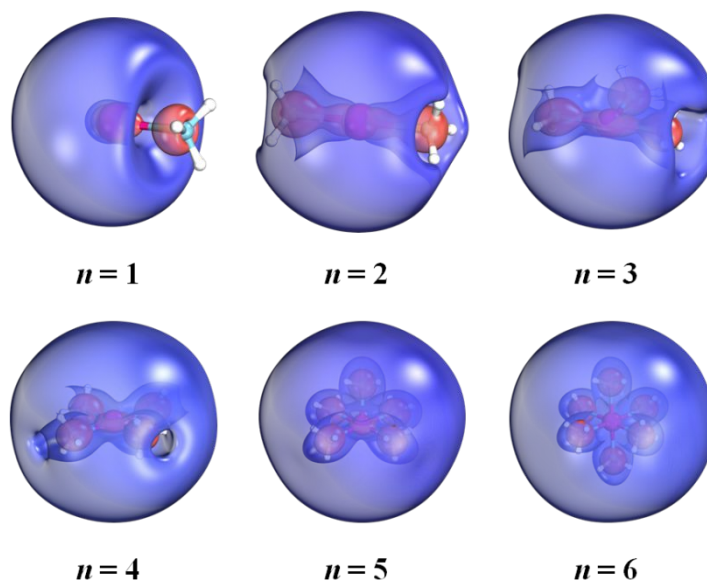


Figure 2. Highest occupied spin-orbitals of ground-state $V(NH_3)_n$ quartets.

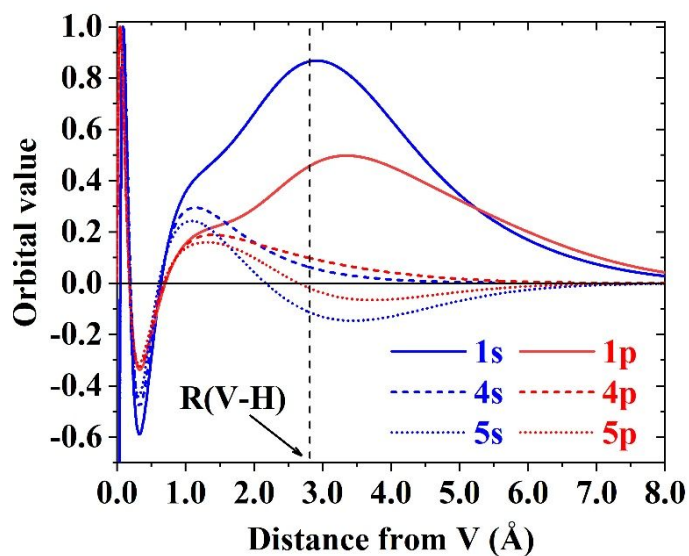


Figure 3. Radial dependence of V 4s, 5s, 4p, 5p and outer 1s and 1p orbitals of $V(NH_3)_6$. The abscissa connects the V nucleus and the center of a N–N–N face. All orbitals are scaled so that the global maximum is set to unity. $R(V-H)$ is the average vanadium-nitrogen distance for $V(NH_3)_6$.

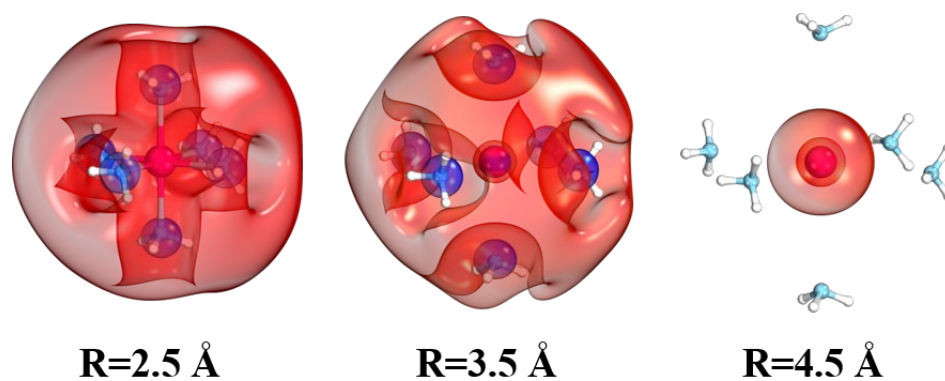


Figure 4. Contours of the highest occupied molecular orbital as a function of the common V-N (R) distance as the six ammonia ligands approach vanadium.

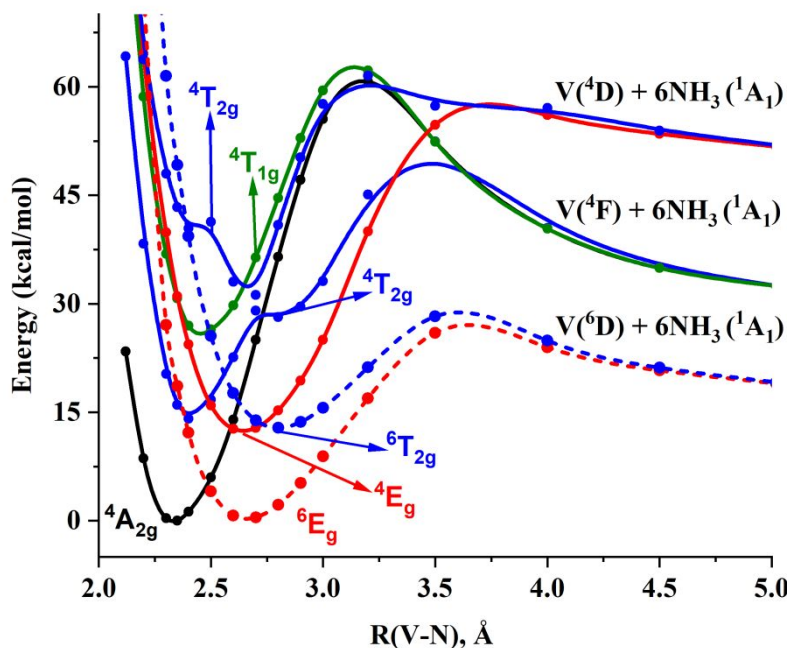


Figure 5. CASSCF PECs with respect to the common V-N distance of six ammonia ligands approaching simultaneously for the first three channels related to $V(^4,6D; 4s^13d^4)$ and $V(^4F; 4s^23d^3)$. Quartets and sextets correspond to solid and dashed lines, respectively. Black, red, blue, green relate to A_{1g} , E_g , T_{2g} , and T_{1g} states.

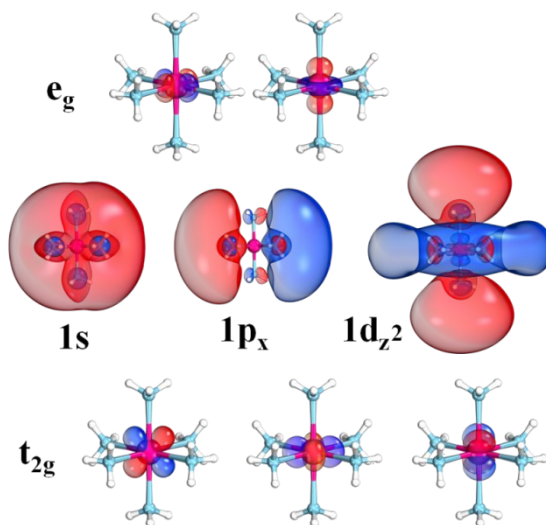


Figure 6. 3d-like (t_{2g} and e_g) and selected outer diffuse molecular orbitals of $V(NH_3)_6$. The orbitals are drawn in energy order: $t_{2g} < \text{outer orbitals} < e_g$. The outer orbitals have been compressed. (See Figure S1 of ESI for a size comparison).

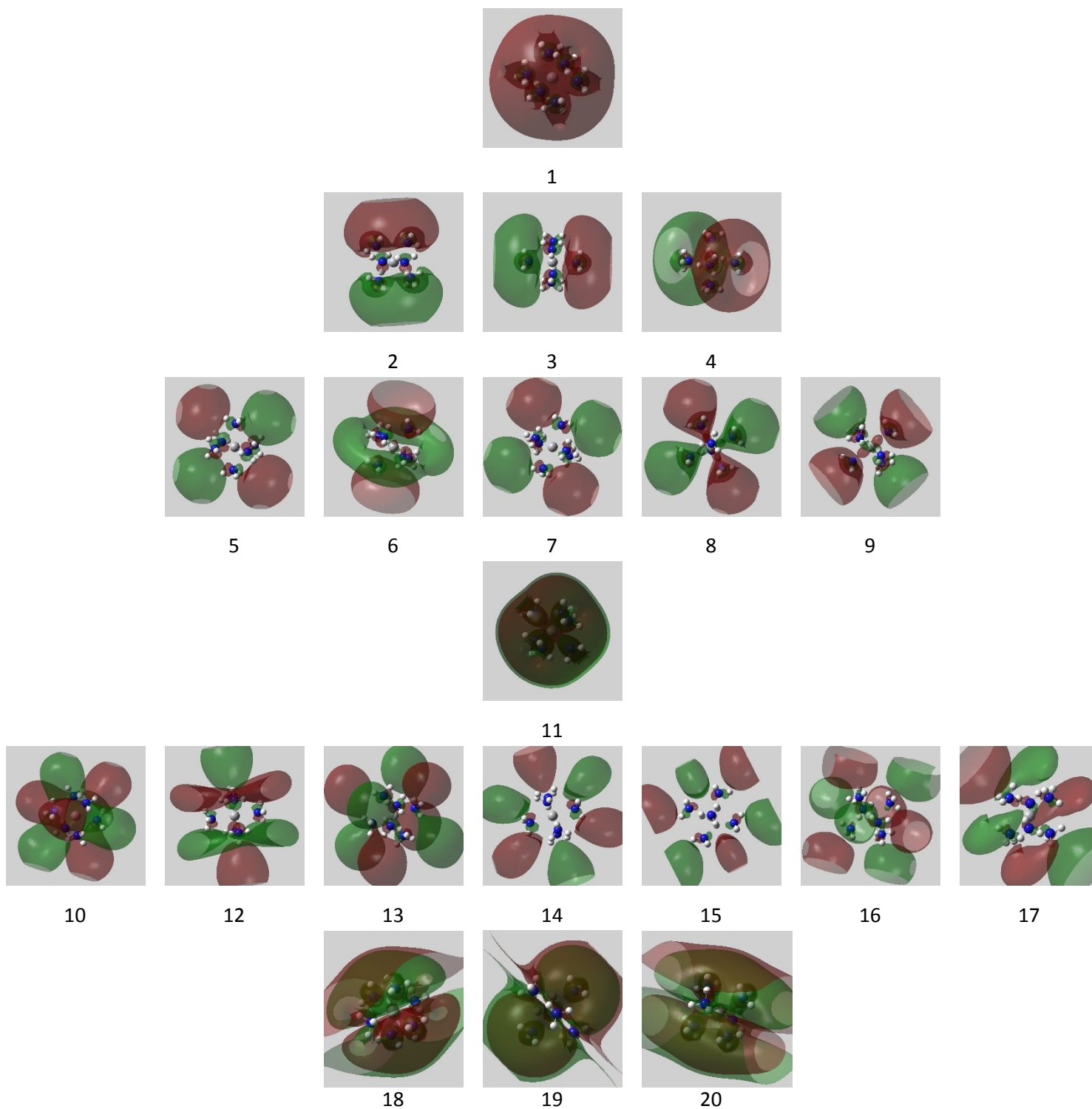


Figure 7. Contours of 1s, 1p, 1d, 2s, 1f, and 2p Dyson orbitals for electron attachment to $V(NH_3)_6^{2+}$ to produce final quintet states. For triplet states, contours are nearly identical. The numerical labels correspond to those in the last column of Table 5.

Table 1. MP2 equilibrium energy E (a.u.), total binding energy $D_{e,\text{tot}}$ (kcal/mol), and dissociation energy of one ammonia ligand D_e (kcal/mol) for $V(\text{NH}_3)_n$.^a

n	$-E$	D_e	$D_{e,\text{tot}}$
0	942.950448		
1	999.429871	13.2	13.2
2	1055.917832	18.6	31.8
3	1112.384277	5.1	36.9
4	1168.875604	20.7	57.5
5	1225.352181	11.4	69.0
6	1281.850740	25.2	94.2

$$^a D_{e,\text{tot}} = E[V(^4\text{F})] + n E[\text{NH}_3] - E[V(\text{NH}_3)_n], D_e = E[V(\text{NH}_3)_{n-1}] + E[\text{NH}_3] - E[V(\text{NH}_3)_n].$$

Table 2. MP2 equilibrium energy E (a.u.), total binding energy $D_{e,\text{tot}}$ (kcal/mol), and dissociation energy of one ammonia ligand D_e (kcal/mol) for $V(\text{NH}_3)_n^+$.

n	$-E$	D_e	$D_{e,\text{tot}}$
0	942.710639		
1	999.242147	45.9	45.9
2	1055.766504	41.4	87.3
3	1112.263367	24.2	111.5
4	1168.763008	25.9	137.4
5	1225.238946	11.0	148.4
6	1281.726482	18.3	166.7

$$^a D_{e,\text{tot}} = E[V(^5\text{F})] + n E[\text{NH}_3] - E[V(\text{NH}_3)_n^+], D_e = E[V(\text{NH}_3)_{n-1}^+] + E[\text{NH}_3] - E[V(\text{NH}_3)_n^+].$$

Table 3. Optimal MP2 V-N and N-H bond lengths (Å), V-N-H angles (°) and relative, adiabatic energies ΔE (eV) of $V(NH_3)_6^{0\pm}$.

Species	V-N ^a	N-H ^a	V-N-H ^b	ΔE ^c
$V(NH_3)_6^{2+}$	2.2860	1.0176	114.3	9.85
$V(NH_3)_6^+$	2.2610	1.0206	113.4	3.50
$V(NH_3)_6$	2.2494	1.0226	113.1	0.00
$V(NH_3)_6^-$	2.2530	1.0219	113.9	-0.48

^a Median value for all bond distances. Deviations are of the 10^{-4} Å order or smaller.

^b Median value for all bond angles. Deviations are about 1.0° for all species.

^c Energy difference from $V(NH_3)_6$ based on P3+ vertical electron binding energies, MP2 C_{2v} - C_1 relaxation energies and B3LYP zero-point energies (see Tables S15 and S16 of ESI).

Table 4. Electronic configuration and vertical excitation energies T_e (eV) at CASSCF and CASPT2 for forty five states of $V(NH_3)_6$.

State ^a	Electronic configuration	Irrep (C_{2v}) ^b	T_e (CASSCF)	T_e (CASPT2)	ΔT_e ^c		
$^4A_{2g}$	$t_{2g}^3 (^4A_{2g}) 1s^2 (^1S)$	B_1	0.000	0.000	0.000		
$^6T_{2u}$	$t_{2g}^3 (^4A_{2g}) 1s^1 1p^1 (^3P)$	B_1	0.377	0.541	0.164		
		A_2	0.384	0.552	0.168		
		A_1	0.393	0.562	0.169		
$^4T_{2u}$	$t_{2g}^3 (^4A_{2g}) 1s^1 1p^1 (^3P)$	B_1	0.388	0.548	0.160		
		A_2	0.395	0.558	0.163		
		A_1	0.403	0.568	0.165		
$^2T_{2u}$	$t_{2g}^3 (^4A_{2g}) 1s^1 1p^1 (^3P)$	B_1	0.394	0.553	0.159		
		A_2	0.401	0.564	0.163		
		A_1	0.410	0.573	0.163		
$4?$	mixture ^d	A_2	0.967	1.282	0.315		
		B_1	0.980	1.298	0.318		
		B_2	1.024	1.342	0.318		
		A_1	1.034	1.307	0.273		
		B_1	1.037	1.342	0.305		
		A_2	1.081	1.231	0.150		
		B_1	1.083	1.319 ^e			
		A_1	1.089	1.256	0.167		
		$^6T_{2g}$	$t_{2g}^3 (^4A_{2g}) 1p^2 (^3P)$	A_2	1.347	1.659	0.312
				B_2	1.356	1.666	0.310
A_1	1.351			1.661	0.310		
$^2T_{2g}$	$t_{2g}^3 (^4A_{2g}) 1p^2 (^3P)$	A_2	1.357	1.666	0.309		
		A_1	1.361	1.668	0.307		
		B_2	1.365	1.673	0.308		
$4?$	mixture ^d	A_2	1.353	1.658	0.305		
		A_1	1.357	1.661	0.304		
		B_2	1.362	1.660	0.298		
		A_2	1.436	1.672 ^e			
		B_1	1.476	1.712 ^e			
		B_2	1.493	1.729 ^e			
		A_1	1.536	1.772 ^e			
		B_1	1.551	1.787 ^e			
		$^6T_{1g} + ^6E_g$	$t_{2g}^3 (^4A_{2g}) 1s^1 1d^1$ (^{3D})	A_2	1.435	1.675	0.240

		B ₁	1.472	1.677	0.205
		B ₂	1.488	1.757	0.269
		A ₁	1.524	1.723	0.199
		B ₁	1.540	1.719	0.179
${}^2T_{1g} + {}^2E_g$	$t_{2g}^3 ({}^4A_{2g}) 1s^1 1d^1$ (3D)	A ₂	1.437	1.668	0.231
		B ₁	1.478	1.677	0.199
		B ₂	1.496	1.762	0.266
		A ₁	1.542	1.746	0.204
		B ₁	1.558	1.740	0.182
${}^4T_{2g}$	$t_{2g}^2 e_g^1 ({}^4T_{2g}) 1s^2 ({}^1S)$	A ₂	1.698	1.751 ^f	
		A ₁	1.704	1.757 ^f	
		B ₂	1.710	1.763 ^f	

^a Electronic terms under O_h obtained based on the electronic configuration.

^b Irreducible representation under C_{2v}; axes are oriented as in Figure 1.

^c $\Delta T_e = T_e(\text{CASPT2}) - T_e(\text{CASSCF})$.

^d These states are mixtures of the $t_{2g}^3 ({}^4A_{2g}) 1s^1 1d^1 ({}^3D)$, $t_{2g}^3 ({}^4A_{2g}) 1p^1 1p^1 ({}^3P, {}^1D, {}^1S)$, and $t_{2g}^3 ({}^4A_{2g}) 1p^1 1d^1$ electronic configurations; see text.

^e Estimated values obtained as $T_e(\text{CASPT2}) = T_e(\text{CASSCF}) + \delta E$, where $\delta E = 0.236$ eV is the average T_e difference for all of the $t_{2g}^3 ({}^4A_{2g})$ of V(NH₃)₆; see text.

^f Estimated values obtained as $T_e(\text{CASPT2}) = T_e(\text{CASSCF}) + \delta E$, where $\delta E = 0.053$ eV is the average T_e difference for all of the $t_{2g}^2 e_g^1 ({}^4T_{2g})$ of V(NH₃)₆⁺; see text.

Table 5. Electronic configuration and vertical excitation energies T_e (eV) at CASSCF, CASPT2, and P3+ for thirty four states of $V(NH_3)_6^+$.

State ^a	Electronic configuration	Irrep (C _{2v}) ^b	T_e (CASSCF)	T_e (CASPT2)	ΔT_e ^c	T_e (P3+)	T_e ^d (C-P3+)	DO # ^e
⁵ A _{2g}	t _{2g} ³ (⁴ A _{2g}) 1s ¹ (² S)	B ₁	0.000	0.004	0.004	0.000	0.000	1
³ A _{2g}	t _{2g} ³ (⁴ A _{2g}) 1s ¹ (² S)	B ₁	0.016	0.000	-0.016	0.012	0.012	1
⁵ T _{2u}	t _{2g} ³ (⁴ A _{2g}) 1p ¹ (² P)	A ₂	0.794	0.972	0.178	0.980	0.998	2
		A ₁	0.801	0.979	0.178	0.987	1.004	3
		B ₁	0.790	0.999	0.209	0.976	0.994	4
³ T _{2u}	t _{2g} ³ (⁴ A _{2g}) 1p ¹ (² P)	A ₂	0.802	0.984	0.182	0.988	1.005	2
		A ₁	0.809	0.990	0.181	0.994	1.012	3
		B ₁	0.798	1.003	0.205	0.984	1.001	4
⁵ T _{2g}	t _{2g} ² e _g ¹ (⁴ T _{2g}) 1s ¹ (² S)	A ₂	1.634	1.692	0.058			
		B ₂	1.646	1.700	0.054			
		A ₁	1.641	1.702	0.061			
³ T _{2g}	t _{2g} ² e _g ¹ (⁴ T _{2g}) 1s ¹ (² S)	A ₂	1.650	1.696	0.046			
		B ₂	1.663	1.702	0.039			
		A ₁	1.658	1.716	0.058			
³ T _{2g} + ³ E _g	t _{2g} ³ (² T _{2g} + ² E _g) 1s ¹ (² S)	A ₁	2.027	1.821	-0.206			
		B ₁	2.027	1.838	-0.189			
		B ₂	2.125	1.902	-0.223			
		A ₂	2.127	1.919	-0.208			
		B ₁	2.127	1.922	-0.205			
¹ T _{2g} + ¹ E _g	t _{2g} ³ (² T _{2g} + ² E _g) 1s ¹ (² S)	B ₁	2.035	1.816	-0.219			
		A ₁	2.035	1.817	-0.218			
		B ₁	2.135	1.916	-0.219			
		B ₂	2.133	1.917	-0.216			
		A ₂	2.135	1.918	-0.217			
⁵ T _{1g} + ⁵ E _g	t _{2g} ³ (⁴ A _{2g}) 1d ¹ (² D)	A ₂	1.568	1.907	0.339	1.912	1.924	5
		B ₁	1.590	1.939	0.349	1.918	1.932	6
		B ₂	1.643	2.007	0.364	2.036	2.052	7
		A ₁	1.650	1.903	0.253	1.928	1.944	8
		B ₁	1.665	1.997	0.332	1.981	1.997	9
³ T _{1g} + ³ E _g	t _{2g} ³ (⁴ A _{2g}) 1d ¹ (² D)	A ₂	1.554	1.891	0.337	1.895	1.900	5
		B ₁	1.580	1.937	0.357	1.909	1.916	6
		A ₁	1.666	1.945	0.279	2.033	2.047	7
		B ₁	1.677	2.012	0.335	1.954	1.972	8
		B ₂	1.642	2.019	0.377	1.996	2.015	9
⁵ A _{1u}	t _{2g} ³ (⁴ A _{2g}) 1f ¹ (² F)	A ₂				2.389	2.387	10

${}^3A_{1u}$	$t_{2g}^3 ({}^4A_{2g}) 1f^1 ({}^2F)$	A_2	2.395	2.393	10
${}^3A_{2g}$	$t_{2g}^3 ({}^4A_{2g}) 2s^1 ({}^2S)$	B_1	2.799	2.816	11
${}^5A_{2g}$	$t_{2g}^3 ({}^4A_{2g}) 2s^1 ({}^2S)$	B_1	2.801	2.818	11
${}^5T_{1u}+{}^5T_{2u}$	$t_{2g}^3 ({}^4A_{2g}) 1f^1 ({}^2F)$	A_1	2.864	2.886	12
		B_2	2.945	2.969	13
		B_1	2.995	3.019	14
		B_1	3.093	3.118	15
		A_1	3.103	3.129	16
		A_2	3.107	3.132	17
${}^3T_{1u}+{}^3T_{2u}$	$t_{2g}^3 ({}^4A_{2g}) 1f^1 ({}^2F)$	A_1	2.865	2.887	12
		B_2	2.936	2.960	13
		B_1	2.996	3.020	14
		B_1	3.093	3.119	15
		A_1	3.107	3.133	16
		A_2	3.108	3.133	17
${}^5T_{2u}$	$t_{2g}^3 ({}^4A_{2g}) 2p^1 ({}^2P)$	A_1	3.209	3.241	18
		A_2	3.216	3.247	19
		B_1	3.215	3.249	20
${}^3T_{2u}$	$t_{2g}^3 ({}^4A_{2g}) 2p^1 ({}^2P)$	A_1	3.218	3.250	18
		A_2	3.226	3.257	19
		B_1	3.228	3.260	20

^a Electronic terms under O_h obtained based on the electronic configuration.

^b Irreducible representation under C_{2v} ; axes are oriented as in Figure 1.

^c $\Delta T_e = T_e(\text{CASPT2}) - T_e(\text{CASSCF})$.

^d The vanadium $3s^23p^6$ electron correlation is included.

^e Numbers in the last column correspond to numerical labels of Dyson orbitals presented in Figure 7.

ASSOCIATED CONTENT

Supporting Information.

AUTHOR INFORMATION

Notes

The authors declare no competing financial interests.

ACKNOWLEDGMENT

The authors are indebted to Auburn University (AU) for financial support. This work was completed in part with resources provided by the AU Hopper Cluster. JVO acknowledges the support of the National Science Foundation through grant CHE-1565760 to Auburn University.

Supporting Information Available: Figure S1 depicts the active orbitals. Optimal geometries and harmonic vibrational frequencies, are listed in Tables S1-S6. P3+ electron binding energies are given in Tables S7-S14. Table S15 lists adiabatic electron binding energies and Table S16 lists absolute energies for all optimal C_{2v} and C_1 structures.

References

1. E. Zurek, P. P. Edwards and R. Hoffmann, *Angew. Chem. Int. Ed.*, 2009, **48**, 8198-8232.
2. C. Combellas, F. Kanoufi and A. Thiebault, *J. Electroanal. Chem.*, 2001, **499**, 144-151.
3. M. Mauksch and S. B. Tsogoeva, *Phys. Chem. Chem. Phys.*, 2018, **XX**, XXXX.
4. Y. Yamamoto, S. Karashima, S. Adachi and T. Suzuki, *J. Phys. Chem. A*, 2016, **120**, 1153-1159.
5. J. A. Walker and D. M. Bartels, *J. Phys. Chem. A*, 2016, **120**, 7240-7247.
6. V. V. Chaban and O. V. Prezhdo, *J. Phys. Chem. B*, 2016, **120**, 2500-2506.
7. A. G. Seel, H. Swan, D. T. Bowron, J. C. Wasse, T. Weller, P. P. Edwards, C. A. Howard and N. T. Skipper, *Angew. Chem. Int. Ed.*, 2017, **56**, 1561-1565.
8. E. Zurek, X. D. Wen and R. Hoffmann, *J. Am. Chem. Soc.*, 2011, **133**, 3535-3547.
9. G. J. Martyna, Z. H. Deng and M. L. Klein, *J. Chem. Phys.*, 1993, **98**, 555-563.
10. I. R. Ariyaratna, F. Pawłowski, J. V. Ortiz and E. Miliordos, *Phys. Chem. Chem. Phys.*, 2018, **20**, 24186-24191.
11. I. R. Ariyaratna, S. N. Khan, F. Pawłowski, J. V. Ortiz and E. Miliordos, *J. Phys. Chem. Lett.*, 2018, **9**, 84-88.
12. T. Sommerfeld and K. M. Dreux, *J. Chem. Phys.*, 2012, **137**, 7.
13. P. Brockhaus, I. V. Hertel and C. P. Schulz, *The Journal of Chemical Physics*, 1998, **110**, 393-402.
14. A. Kramida, Ralchenko, Yu., Reader, J., and NIST ASD Team (2018). NIST Atomic Spectra Database (ver. 5.5.2), [Online]. Available: <https://physics.nist.gov/asd> NIST, (accessed 2018, November 1).
15. A. D. Becke, *J. Chem. Phys.*, 1993, **98**, 5648-5652.
16. C. T. Lee, W. T. Yang and R. G. Parr, *Phys. Rev. B*, 1988, **37**, 785-789.
17. N. B. Balabanov and K. A. Peterson, *J. Chem. Phys.*, 2005, **123**, 064107.
18. R. A. Kendall, T. H. Dunning and R. J. Harrison, *J. Chem. Phys.*, 1992, **96**, 6796-6806.
19. T. H. Dunning, *J. Chem. Phys.*, 1989, **90**, 1007-1023.
20. M. H. Palmer, S. V. Hoffmann, N. C. Jones, M. Coreno, M. d. Simone and C. Grazioli, *J. Chem. Phys.*, 2018, **148**, 214304.
21. H.-J. Werner, P. J. Knowles, G. Knizia, F. R. Manby, M. {Schütz}, P. Celani, W. Györffy, D. Kats, T. Korona, R. Lindh, A. Mitrushenkov, G. Rauhut, K. R. Shamasundar, T. B. Adler, R. D. Amos, A. Bernhardsson, A. Berning, D. L. Cooper, M. J. O. Deegan, A. J. Dobbyn, F. Eckert, E. Goll, C. Hampel, A. Hesselmann, G. Hetzer, T. Hrenar, G. Jansen, C. Köppl, Y. Liu, A. W. Lloyd, R. A. Mata, A. J. May, S. J. McNicholas, W. Meyer, M. E. Mura, A. Nicklass, D. P. O'Neill, P. Palmieri, D. Peng, K. Pflüger, R. Pitzer, M. Reiher, T. Shiozaki, H. Stoll, A. J. Stone, R. Tarroni, T. Thorsteinsson and M. Wang, *Journal*, 2015.
22. G. Ghigo, B. O. Roos and P. A. Malmqvist, *Chem. Phys. Lett.*, 2004, **396**, 142-149.
23. B. O. Roos and K. Andersson, *Chem. Phys. Lett.*, 1995, **245**, 215-223.
24. H. H. Corzo and J. V. Ortiz, in *Adv. Quantum Chem.*, eds. J. R. Sabin and E. J. Brändas, Academic Press, 2017, vol. 74, pp. 267-298.
25. M. J. Frisch, G. W. Trucks, H. B. Schlegel, G. E. Scuseria, M. A. Robb, J. R. Cheeseman, G. Scalmani, V. Barone, G. A. Petersson, H. Nakatsuji, X. Li, M. Caricato, A. V. Marenich, J. Bloino, B. G. Janesko, R. Gomperts, B. Mennucci, H. P. Hratchian, J. V. Ortiz, A. F. Izmaylov, J. L. Sonnenberg, Williams, F. Ding, F. Lipparini, F. Egidi, J.

- Goings, B. Peng, A. Petrone, T. Henderson, D. Ranasinghe, V. G. Zakrzewski, J. Gao, N. Rega, G. Zheng, W. Liang, M. Hada, M. Ehara, K. Toyota, R. Fukuda, J. Hasegawa, M. Ishida, T. Nakajima, Y. Honda, O. Kitao, H. Nakai, T. Vreven, K. Throssell, J. A. Montgomery Jr., J. E. Peralta, F. Ogliaro, M. J. Bearpark, J. J. Heyd, E. N. Brothers, K. N. Kudin, V. N. Staroverov, T. A. Keith, R. Kobayashi, J. Normand, K. Raghavachari, A. P. Rendell, J. C. Burant, S. S. Iyengar, J. Tomasi, M. Cossi, J. M. Millam, M. Klene, C. Adamo, R. Cammi, J. W. Ochterski, R. L. Martin, K. Morokuma, O. Farkas, J. B. Foresman and D. J. Fox, *Journal*, 2016.
26. C. S. Feigerle, R. R. Corderman, S. V. Bobashev and W. C. Lineberger, *J. Chem. Phys.*, 1981, **74**, 1580-1598.

TOC GRAPHIC

